Extremophiles (2020) 24:551–564
https://doi.org/10.1007/s00792-020-01175-z

ORIGINAL PAPER

Carbon monoxide-dependent transcriptional changes in a thermophilic, carbon monoxide-utilizing, hydrogen-evolving bacterium *Calderihabitans maritimus* KKC1 revealed by transcriptomic analysis

Masao Inoue[1] · Hikaru Izumihara[1] · Yuto Fukuyama[1] · Kimiho Omae[1] · Takashi Yoshida[1] · Yoshihiko Sako[1]

Received: 6 March 2020 / Accepted: 27 April 2020 / Published online: 9 May 2020
© The Author(s) 2020

Abstract

Calderihabitans maritimus KKC1 is a thermophilic, carbon monoxide (CO)-utilizing, hydrogen-evolving bacterium that harbors seven *cooS* genes for anaerobic CO dehydrogenases and six *hyd* genes for [NiFe] hydrogenases and capable of using a variety of electron acceptors coupled to CO oxidation. To understand the relationships among these unique features and the transcriptional adaptation of the organism to CO, we performed a transcriptome analysis of *C. maritimus* KKC1 grown under 100% CO and N_2 conditions. Of its 3114 genes, 58 and 32 genes were significantly upregulated and downregulated in the presence of CO, respectively. A *cooS–ech* gene cluster, an "orphan" *cooS* gene, and bidirectional *hyd* genes were upregulated under CO, whereas hydrogen-uptake *hyd* genes were downregulated. Transcriptional changes in anaerobic respiratory genes supported the broad usage of electron acceptors in *C. maritimus* KKC1 under CO metabolism. Overall, the majority of the differentially expressed genes were oxidoreductase-like genes, suggesting metabolic adaptation to the cellular redox change upon CO oxidation. Moreover, our results suggest a transcriptional response mechanism to CO that involves multiple transcription factors, as well as a CO-responsive transcriptional activator (CooA). Our findings shed light on the diverse mechanisms for transcriptional and metabolic adaptations to CO in CO-utilizing and hydrogen-evolving bacteria.

Keywords Carbon monoxide · Hydrogen · Hydrogenase · Energy conservation · Transcriptome · RNA-seq

Abbreviations

CODH	Carbon monoxide dehydrogenase
Ni-CODH	Anaerobic Ni-containing CODH
ECH	Energy converting hydrogenase
WLP	Wood–Ljungdahl pathway
Kor	2-Oxoglutarate:ferredoxin oxidoreductase
RNA-seq	RNA sequencing
RT-ddPCR	Reverse transcriptase droplet digital polymerase chain reaction
NCBI	The National Centre for Biotechnology Information
DEG	Differentially expressed gene
COG	Cluster of orthologous groups
Fdh	Periplasmic formate dehydrogenase
Nap	Periplasmic nitrate reductase
Dsr	Dissimilatory sulfite reductase
MHC	Extracellular multiheme cytochromes *c*
GS	Glutamine synthetase
GOGAT	Glutamate synthase
SCS	Succinyl-CoA synthetase
DCCP	Double-cubane cluster protein

Communicated by H. Atomi.

Electronic supplementary material The online version of this article (https://doi.org/10.1007/s00792-020-01175-z) contains supplementary material, which is available to authorized users.

✉ Yoshihiko Sako
sako@kais.kyoto-u.ac.jp

[1] Graduate School of Agriculture, Kyoto University, Kitashirakawa Oiwake-cho, Sakyo-ku, Kyoto 606-8502, Japan

Introduction

Carbon monoxide (CO) is used as an energy source by CO-oxidizing microbes (carboxydotrophs) because of its low redox potential (Ragsdale 2004; Oelgeschläger and Rother 2008; Sokolova et al. 2009; Diender et al.

2015). Carboxydotrophs harness CO dehydrogenases (CODHs) for CO utilization by catalyzing the reaction $CO + H_2O \rightleftharpoons CO_2 + 2H^+ + 2e^-$ (Ragsdale 2004; Oelgeschläger and Rother 2008). CODHs are divided into two families: anaerobic Ni-containing CODHs (Ni-CODHs) and aerobic molybdenum- and copper-containing CODHs (Can et al. 2014; Hille et al. 2015). Unlike aerobic CODHs, Ni-CODHs can reduce ferredoxin and thereby utilize various types of terminal electron acceptors, such as protons, CO_2, sulfate, and ferric iron [Fe(III)] (Oelgeschläger and Rother 2008; Sokolova et al. 2009; Diender et al. 2015). Because of this unique feature of Ni-CODHs, physiologically diverse anaerobic carboxydotrophs have been described, such as hydrogenogens, acetogens, methanogens, sulfate reducers, and Fe(III) reducers (Oelgeschläger and Rother 2008; Sokolova et al. 2009; Diender et al. 2015).

Hydrogenogenic carboxydotrophs couple CO oxidation with proton reduction to produce hydrogen (H_2), during which the proton- or sodium-motive force is generated with residual energy via a Ni-CODH/energy converting hydrogenase (ECH) complex (Singer et al. 2006; Schut et al. 2016; Schoelmerich and Müller 2019). CO-dependent H_2 production by hydrogenogenic carboxydotrophs is considered a "safety valve" to reduce toxic CO and supply H_2, which is an energy source for H_2-utilizing microbial communities (Techtmann et al. 2009). Hydrogenogenic carboxydotrophs are generally divided into three groups in their phylogeny: Firmicutes, Proteobacteria, and Archaea (Diender et al. 2015; Inoue et al. 2019). In Firmicutes, the Clostridia includes various types of thermophilic, hydrogenogenic carboxydotrophs that harbor multiple *cooS* genes and feature the Wood–Ljungdahl pathway (WLP) for carbon fixation (Techtmann et al. 2012; Shin et al. 2016; Inoue et al. 2019).

The functions of these *cooS* genes have been predicted from their genomic contexts such as ECH, WLP, and ferredoxin–NAD(P)H oxidoreductase (Techtmann et al. 2012; Inoue et al. 2019), which are presumed to be regulated by CO-responsive transcription factors, such as CooA and RcoM (Shelver et al. 1995; Komori et al. 2007; Kerby et al. 2008). However, recent studies of two hydrogenogenic carboxydotrophs, *Carboxydothermus pertinax* and *Thermoanaerobacter kivui*, show that the enzymatic coupling of *cooS* and *ech* genes that are distantly encoded in their respective genomes enables CO-dependent H_2 production (Fukuyama et al. 2018, 2019a; Schoelmerich and Müller 2019). Moreover, *cooS* expression is upregulated in the presence of CO, despite the fact that no sequence motif is recognized by the CO-responsive transcriptional activator CooA in *C. pertinax* (Fukuyama et al. 2018, 2019a). Similarly, *ech* expression is upregulated in the presence of CO, although the genome does not encode any previously described CO-responsive transcription factors in *T. kivui* (Schoelmerich and Müller 2019). These studies suggest that there are previously unknown transcriptional response mechanisms to CO. Therefore, the direct observation of transcriptional, proteomic, and metabolic changes under CO is required to understand the metabolisms of hydrogenogenic carboxydotrophic bacteria.

Calderihabitans maritimus KKC1 is a thermophilic, obligately anaerobic, hydrogenogenic, carboxydotrophic bacterium in the Clostridia, closely related to *Moorella*, and was isolated from a core sample taken from marine sediment in the Kikai Caldera, Japan (Yoneda et al. 2013). *C. maritimus* KKC1 can grow anaerobically on 100% CO while producing H_2 and CO_2 with or without additional electron acceptors such as thiosulfate, sulfite, ferric citrate, amorphous Fe(III) oxide, Fe_2O_3, or fumarate, and on organic compounds, such as pyruvate, in the presence of thiosulfate. *C. maritimus* KKC1 requires yeast extract for CO-dependent growth unlike chemolithoautotrophic, hydrogenogenic carboxydotrophs, such as *Moorella stamsii* and *Carboxydothermus hydrogenoformans*, and is unable to grow with H_2 and CO_2 unlike chemolithoautotrophic acetogens, such as *Moorella thermoacetica* (Svetlichny et al. 1991; Drake and Daniel 2004; Alves et al. 2013; Yoneda et al. 2013). The draft genome of *C. maritimus* KKC1 encodes six *cooS* genes that are categorized by their genomic contexts, as follows: *cooS1* (KKC1_RS04465), WLP; *cooS2* (KKC1_RS06675), ECH; *cooS3* (KKC1_RS06585), ferredoxin-NAD(P)H oxidoreductase; *cooS4* (KKC1_RS12505), a cysteine synthase and ABC transporter; *cooS5* (KKC1_RS04925), 2-oxoglutarate:ferredoxin oxidoreductase (Kor); and *cooS6* (KKC1_RS10495), CooA (Omae et al. 2017). These six *cooS* genes harbor the complete sequence motifs that form three types of metal clusters for catalysis, although *cooS1* is frame-shifted like other hydrogenogenic, carboxydotrophic *Moorella* and *Carboxydothermus* species possibly as a result of cultivation at high CO concentrations (Wu et al. 2005; Omae et al. 2017; Poehlein et al. 2018; Fukuyama et al. 2018, 2019b). To the best of our knowledge, the genome contains the highest number of *cooS* genes (Omae et al. 2017; Toshchakov et al. 2018) and encodes six hydrogenase gene clusters that include two *ech* gene clusters, a *coo*-type gene cluster (*ech1*, KKC1_RS06640–KKC1_RS06665) with *cooS2*, and a *hyc*/*hyf*-type gene cluster (*ech2*, KKC1_RS01155–KKC1_RS01200) with putative formate dehydrogenase genes (Omae et al. 2017). The genome only harbors one *cooA* gene as a CO-responsive transcription factor.

The multiplicity of Ni-CODHs and hydrogenases and the broad usage of electron acceptors in *C. maritimus* KKC1 suggest genomic adaptation for its carboxydotrophic growth (Yoneda et al. 2013; Omae et al. 2017); however, its metabolic and transcriptional responses to CO remain largely unknown. In this study, we performed a transcriptome analysis of *C. maritimus* KKC1 grown in the presence or absence of CO using RNA sequencing (RNA-seq). Under

CO conditions, we found the evidence of transcriptional changes for Ni-CODHs and hydrogenases, and for anaerobic respiration, carbon and nitrogen metabolism, and transcription factors. We suggest that the transcriptional response mechanism to CO involves multiple transcription factors.

Materials and methods

Cultivation of *C. maritimus* KKC1

Calderihabitans maritimus KKC1 was cultured in modified NBRC 1251 medium, pH 7.5 at 65 °C under 100% CO or 100% N_2 gas as previously described with slight modification (Yoneda et al. 2013). The medium contained 1 g sodium pyruvate, 1 g $Na_2S_2O_3{\cdot}5H_2O$, 50 mg yeast extract, 16 g NaCl, 3.9 g $MgSO_4{\cdot}7H_2O$, 3.9 g $MgCl_2{\cdot}6H_2O$, 0.14 g $CaCl_2{\cdot}2H_2O$, 0.65 g KCl, 0.5 g $NaHCO_3$, 0.1 g NH_4Cl, 0.1 g KH_2PO_4, 0.1 g NaBr, 10 mg Na_2SiO_3, 30 mg H_3BO_3, 15 mg $SrCl_2{\cdot}6H_2O$, 6.6 mg $FeCl_3$, 0.05 mg KI, 0.05 mg $NaNO_3$, 10 mL trace mineral solution SL-4 (Pfennig and Lippert 1966), 1.0 mL vitamin solution (Wolin et al. 1963), 0.5 mg resazurin, and 0.1 g $Na_2S{\cdot}9H_2O$ per liter. Cultivation was performed in 100 mL of medium in a 250-mL bottle sealed with a rubber stopper and a polypropylene screw cap. The cells grown under 100% N_2 gas were inoculated at 10^5–10^6 cells/mL into the fresh media under both 100% CO and 100% N_2 gas conditions with three biological replicates. Cell growth was determined using an S3e Cell Sorter (Bio-Rad, Hercules, CA, USA) by counting the number of fluorescent signals from SYBR Green I-stained cells. Consumption of CO and evolution of H_2 were analyzed by a GC-2014 gas chromatography system (Shimadzu, Kyoto, Japan) equipped with a thermal conductivity detector and a Shincarbon ST packed column (Shinwa Chemical Industries, Kyoto, Japan) using argon as the carrier gas. For RNA extraction, cells were collected on a 0.22-µm Durapore membrane filter (Merck Millipore, Burlington, MA, USA) at the late-exponential phase (Fig. 1a), and then stored in RNA*later* RNA Stabilization Reagent (Qiagen, Hilden, Germany) at − 85 °C until RNA extraction.

RNA isolation and cDNA synthesis

RNA isolation and cDNA synthesis were performed, as previously described (Fukuyama et al. 2018, 2019a). Total RNA was extracted using a mirVana miRNA Extraction Kit (Ambion, Austin, TX, USA), and the remaining genomic DNA was removed using TURBO DNase (Ambion). Total RNA was then purified using Agencourt RNAClean XP beads (Beckman Coulter, Brea, CA, USA), and quantified and quality controlled using a Qubit RNA HS Assay Kit (Invitrogen, Carlsbad, CA, USA) and an Agilent RNA 6000 Pico Kit on an Agilent 2100 Bioanalyzer (Agilent Technologies, Santa Clara, CA, USA). For RNA-seq analysis, rRNA was removed from the purified total RNA using a Ribo-Zero rRNA Removal Kit for Bacteria (Illumina, San Diego, CA, USA), and double-stranded cDNA was synthesized using a PrimeScript Double Strand cDNA Synthesis Kit (Takara, Shiga, Japan). For reverse transcriptase droplet digital polymerase chain reaction (RT-ddPCR), single-stranded cDNA was synthesized using a SuperScript III First-Strand Synthesis System (Invitrogen).

RNA-seq and data analysis

A DNA library for RNA-seq was prepared using a Nextera XT DNA Library Prep Kit (Illumina) with two biological replicates. The library was quantified and quality controlled using KAPA Library Quantification Kits (KAPA Biosystems, Wilmington, MA, USA) on a Thermal Cycler Dice Real Time System Single (Takara) and an Agilent High Sensitivity DNA Kit on an Agilent 2100 Bioanalyzer (Agilent Technologies). Sequencing was performed on the Illumina MiSeq instrument with an MiSeq Reagent Kit v3 (150 cycles), which generated 15,716,607 paired-end reads.

Quality filtering was performed using an FASTX-Toolkit version 0.0.14 (https://hannonlab.cshl.edu/fastx_toolkit/), with the reads being Q30 for > 80% of the bases. Reads from the remaining rRNA were removed using a BLASTn search (Camacho et al. 2009). The filtered reads were mapped onto the draft genome sequence (GCF_002207765.1) of *C. maritimus* KKC1 obtained from the National Centre for Biotechnology Information (NCBI) assembly database (NCBI Resource Coordinators 2018) using HISAT2 version 2.1.0 (Kim et al. 2015). The mapped data were checked using SAMtools version 0.1.19 (Li et al. 2009), and mapped reads per gene were counted using featureCounts from the Subread package version 1.6.3 (Liao et al. 2014). Normalization and differential expression analysis were performed using the R package edgeR version 3.22.5 (Robinson et al. 2009). Differentially expressed genes (DEGs) were identified using the functions "glmQLFit" and "glmTreat" with a fold-change significantly greater than 1.5 at a false discovery rate of ≤ 0.001. The read processing and data set statistics for differential expression analysis are summarized in Tables S1 and S2, respectively.

Functional annotation of the DEGs was performed automatically using EggNOG-mapper version 1.0.3 in HMMER mapping mode (Huerta-Cepas et al. 2017) and RAST server version 2.0 with RASTtk pipeline (Brettin et al. 2015). Annotation was manually confirmed using a BLASTp search (Camacho et al. 2009). Pathway analysis was performed using the Kyoto Encyclopedia of Genes and Genomes mapper version 3.2 (Kanehisa et al. 2012). N-terminal signal sequences were predicted using SignalP server version 5.0

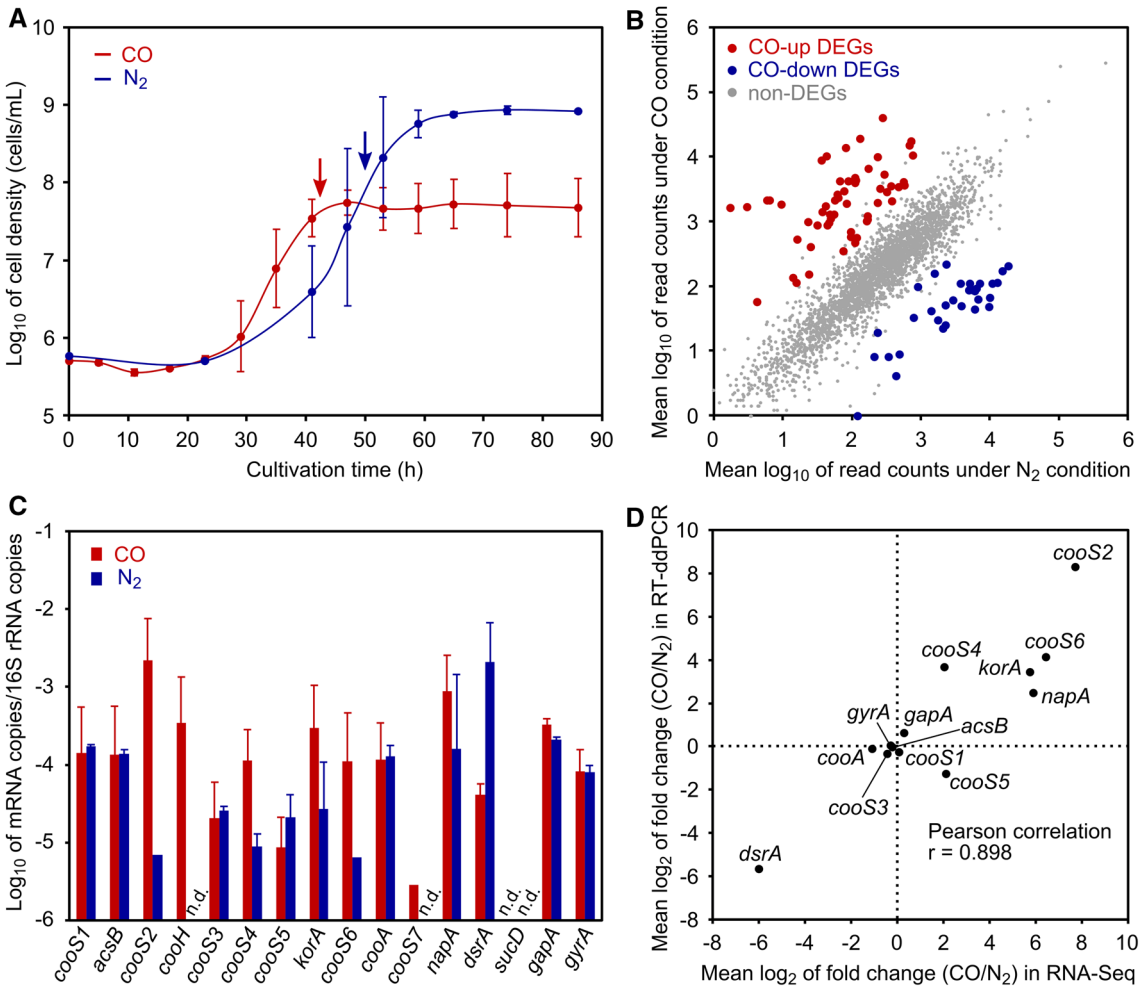

Fig. 1 Overview of RNA-seq and RT-ddPCR datasets. **a** Growth curves of *C. maritimus* KKC1 in the presence (red) or absence (blue) of CO. The mean values of log10-transformed cell densities are plotted. Error bars indicate the standard deviation from three biological replicates. **b** Plots of read counts from genes in the presence or absence of CO. The mean values of log10-transformed read counts from two biological replicates are plotted. Upregulated DEGs in the presence of CO, downregulated DEGs, and non-DEGs are colored red, blue, and gray, respectively. **c** mRNA quantification by RT-ddPCR. The mean values of log10-transformed relative abundances of mRNA relative to 16S rRNA are shown. Values below the lower detection limit were omitted, although all samples were quantified with three biological replicates. Error bars indicate the standard deviation only when at least two values were above lower detection limit. **d** Comparison of fold-change values between RNA-seq and RT-ddPCR data. The mean values of log2-transformed fold changes of each gene are plotted. *n.d.* not detected

(Almagro Armenteros et al. 2019), and hydrogenase annotation was performed using HydDB server (Søndergaard et al. 2016).

Prediction of transcriptional units and identification of transcription-factor-binding motifs

A unit of polycistronically transcribed genes, including DEGs, was manually predicted by checking the read alignments against the draft genome sequence of *C. maritimus* KKC1 using Integrative Genomics Viewer version 2.4.16 (Thorvaldsdóttir et al. 2013) (Table S3). The transcriptional unit comprised continuous same-stranded genes with continuous- and constant-read alignments. To discover sequence motifs in the upstream regions of DEGs, 300-bp upstream sequences from the start codon of the first gene in the transcriptional unit were curated from the genome sequence. Sequence motifs were searched using MEME version 4.12.0 (Bailey et al. 2009), and sequence logos were created using WebLogo version 2.8.2 (Crooks et al. 2004).

RT-ddPCR

To validate the RNA-seq data, RT-ddPCR was performed using a QX200 Droplet Digital PCR System (Bio-Rad) with three biological replicates. Each ddPCR mixture comprised

10 µL of 2 × ddPCR EvaGreen Supermix (Bio-Rad), 0.4 µL of 5 µM primer mix, and 1 µL of appropriately diluted cDNA in a final volume of 20 µL. Droplets were generated using a Droplet Generator (Bio-Rad) with 70 µL of Droplet Generator Oil for EvaGreen (Bio-Rad), and then transferred to a 96-well PCR plate (Eppendorf, Hamburg, Germany) and heat sealed. PCR amplification was performed on a TaKaRa PCR Thermal Cycler Dice *Touch* at 95 °C for 10 min followed by 40 cycles at 94 °C for 30 s and 58 °C for 60 s, one cycle at 98 °C for 10 min, and ending at 8 °C. After amplification, fluorescent signals from the droplets in each well were automatically measured using a Droplet Reader (Bio-Rad).

ddPCR data were analyzed using QuantaSoft software version 1.7.4 (Bio-Rad). To separate positive and negative droplets, thresholds of the fluorescent signals were manually set. The number of target DNA molecules in the reaction mixture was determined from the ratio of positive to total droplets. Data were quality controlled with > 10,000 total droplets in each sample and < 10 positive droplets in the negative control, except for the *korA* primers (< 20 positive droplets in the negative control). The lower limit of detection was set at > 10 positive droplets, except for the *korA* primers (> 20 positive droplets). To compare expression levels in different samples, concentrations of the target genes were normalized against the concentrations of 16S rRNA. All primers used for ddPCR were quality controlled with the lengths and melting curves of the products checked by agarose gel electrophoresis and real-time PCR, respectively (Table S4).

Data availability

The raw reads for RNA-Seq and the gene-expression profiles have been deposited in the NCBI/ENA/DDBJ Sequence Read Archive under accession number DRA008406.

Results

Overview of RNA-seq analysis

We performed RNA-seq experiments for late-exponential cultures of *C. maritimus* KKC1 grown under 100% CO and N_2 gas conditions in biological duplicates (Fig. 1a). To enable growth under N_2 conditions, pyruvate and thiosulfate were added to the medium under both gas conditions. Under CO conditions, conversion of ~ 10% of CO to H_2 was observed at the sampling point by gas chromatography (data not shown). Over 3 million high-quality RNA-seq reads in each sample were mapped with sufficient coverages (> 100 × mean coverage in each sample) and mapping efficiencies (> 80% in each sample) (Table S1). The biological replicates for the CO and N_2 conditions of the RNA-seq experiments were highly reproducible with Pearson's correlation coefficients of 0.968 and 0.970, respectively (Fig. S1).

Normalization and differential gene-expression analysis were performed using mapped RNA-seq data. Of the 3,114 genes in *C. maritimus* KKC1, 90 were differentially expressed between the two conditions, with these DEGs including 58 upregulated and 32 downregulated genes in the presence of CO and $\log_2$-fold changes for CO/N_2 ranging from 2.57 to 10.3 and from − 7.16 to − 2.68, respectively (Fig. 1b and Table S2). Approximately 60% of the upregulated and ~ 70% of the downregulated DEGs in the presence of CO were grouped into the "metabolism" categories of Clusters of Orthologous Groups (COGs) (Galperin et al. 2015), with > 40% of both upregulated and downregulated DEGs were grouped in the COG functional category "C" (energy production and conversion) (Table S2). These data are comparable with those obtained by a recent RNA-seq study of *C. pertinax* (Fukuyama et al. 2019a).

The expression levels of the seven DEGs and eight non-DEGs, including *cooS* genes (*cooS1* through *cooS6*) and house-keeping genes (*gapA* and *gyrA*), were confirmed by RT-ddPCR (Fig. 1c). The *C. maritimus* KKC1genome also contains two partial *cooS*-like gene fragments (KKC1_RS14835 and KKC1_RS01100) (Omae et al. 2017) sharing 65 bp and 16 aa perfect matches encoding one protein (hereafter designated as CooS7). The expression level of *cooS7* judged as non-DEGs was also tested. The fold-change values in RNA-seq and RT-ddPCR data were highly correlated, with a Pearson's correlation coefficient of 0.898 (Fig. 1d), suggesting that our RNA-seq data captured the precise transcriptional changes between CO and N_2 conditions.

CO-dependent differential expression of multiple genes encoding Ni-CODHs and hydrogenases

We first focused on transcriptional changes in Ni-CODHs and hydrogenases, which are responsible for carboxydotrophic and hydrogenogenic growth. Of the seven *cooS* genes in *C. maritimus* KKC1, only *cooS2* and *cooS6* were identified as upregulated DEGs in the presence of CO (Fig. 2; Tables 1 and S2). All of the genes in the *cooS2–ech1* (*coo*-type) gene cluster (KKC1_RS06640–KKC1_RS06680) were upregulated DEGs in the presence of CO, indicating that the Ni-CODH/ECH (Coo-type) complex was responsible for CO-dependent H_2 production, similar to other hydrogenogenic carboxydotrophs (Soboh et al. 2002; Singer et al. 2006; Schut et al. 2016; Schoelmerich and Müller 2019). Conversely, the expression level of the *ech2* (*hyc*/*hyf*-type) gene cluster (KKC1_RS01155–KKC1_RS01200) was unchanged under CO conditions, indicating a potential function with its gene neighbor encoding the putative formate dehydrogenase.

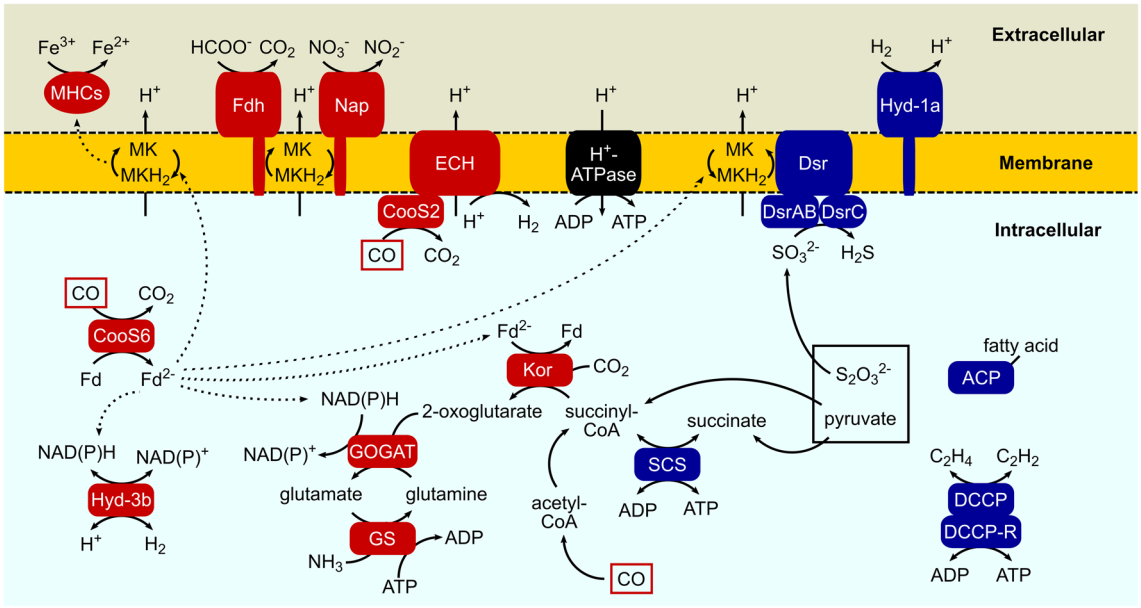

Fig. 2 Schematic representation of metabolic pathways in *C. maritimus* KKC1 with DEGs. Only pathways discussed in the text are shown. Protein machineries with upregulated and downregulated DEGs in the presence of CO are colored red and blue, respectively. ATP synthase (H^+-ATPase) is colored black. Dotted arrows indicate the possible pathways of electron flow from CO oxidation. *MK* menaquinone, *MKH_2* menaquinol

Table 1 List of Ni-CODHs and hydrogenases identified in DEGs

Functional group	Locus tag	Log_2FC	Annotation	COG number (category)[a]
CooS2/Ech1	KKC1_RS06640	8.4	CooM	COG0651,COG1007 (C)
CooS2/Ech1	KKC1_RS06645	7.9	CooK	COG0650 (C)
CooS2/Ech1	KKC1_RS06650	9.5	CooL	COG3260 (C)
CooS2/Ech1	KKC1_RS06655	8.8	CooX	COG1143 (C)
CooS2/Ech1	KKC1_RS06660	10.3	CooU	(C)
CooS2/Ech1	KKC1_RS06665	9.0	CooH	COG3261 (C)
CooS2/Ech1	KKC1_RS06670	8.5	CooF	COG1142 (C)
CooS2/Ech1	KKC1_RS06675	7.7	CooS	COG1151 (C)
CooS2/Ech1	KKC1_RS06680	6.0	CooC	COG3640 (D)
CooS6	KKC1_RS10495	6.5	CooS	COG1151 (C)
Hyd-3b	KKC1_RS10615	5.0	Group 3b Ni,Fe-hydrogenase beta subunit	COG1145 (C)
Hyd-3b	KKC1_RS10620	5.0	Group 3b Ni,Fe-hydrogenase gamma subunit	COG0543 (C)
Hyd-3b	KKC1_RS10625	4.8	Group 3b Ni,Fe-hydrogenase small subunit	COG1941 (C)
Hyd-3b	KKC1_RS10630	5.8	Group 3b Ni,Fe-hydrogenase large subunit	COG3259 (C)
Hyd-3b	KKC1_RS10635	4.8	Ni,Fe-hydrogenase maturation factor	(O)
Hyd-1a	KKC1_RS00385	− 5.2	Group 1a Ni,Fe-hydrogenase small subunit	COG1740 (C)
Hyd-1a	KKC1_RS00390	− 4.1	Group 1a Ni,Fe-hydrogenase large subunit	COG0374 (C)
Hyd-1a	KKC1_RS00395	− 4.8	Group 1a Ni,Fe-hydrogenase cytochrome *b* subunit	COG1969 (C)
Hyd-1a	KKC1_RS00400	− 4.1	Ni,Fe-hydrogenase maturation factor	COG0680 (O)

[a]COG number and category were annotated by EggNOG mapper. Note that some COG categories were annotated, even when COG numbers were not annotated

FC fold change

cooS6 expression was upregulated, whereas that of an adjacent upstream gene (*cooA*) was unchanged, and the other five *cooS* genes were not identified as DEGs (Figs. 1d and 2; Table 1 and S2). It should be noted that the expression level of *cooS4* was higher in the presence of CO in both RNA-Seq and RT-ddPCR experiments albeit a non-DEG (Fig. 1c and d; Table S2). RNA-Seq and RT-ddPCR revealed that *cooS1* and *acsB*, which are involved in WLP, were highly expressed in the presence and absence of CO (although *cooS1* is frame-shifted) (Fig. 1c and Table S2), similar to results from recent RNA-seq data for *C. pertinax* (Fukuyama et al. 2019a). These data suggested that gene transcription for WLP is unchanged between CO and N_2 conditions in these hydrogenogenic, carboxydotrophic bacteria.

Two of the four putative [NiFe] hydrogenase genes other than the two *ech* genes in *C. maritimus* KKC1 were identified as DEGs (Fig. 2; Table 1 and S2). Under CO conditions, the expression levels of *hyd-3b* genes (KKC1_RS10620–KKC1_RS10635) encoding group 3b [NiFe] hydrogenase catalytic subunits and their maturation protease were upregulated, whereas those of *hyd-1a* genes (KKC1_RS00385–KKC1_RS00400) encoding group 1a [NiFe] hydrogenase catalytic subunits, a cytochrome *b* subunit, and their maturation protease were downregulated. The group 3b [NiFe] hydrogenase is a cytoplasmic, bidirectional hydrogenase that directly couples NADPH oxidation to H_2 evolution (Greening et al. 2016; Søndergaard et al. 2016), although it remains unclear whether NADPH is utilized by this enzyme in *C. maritimus* KKC1. Conversely, the group 1a [NiFe] hydrogenase is a periplasmic, unidirectional H_2-uptake hydrogenase, and the cytochrome *b* subunit is considered a putative electron carrier, as are other group 1 hydrogenases (Greening et al. 2016; Søndergaard et al. 2016); however, a terminal electron acceptor has not been identified in *C. maritimus* KKC1.

Transcriptional changes in anaerobic respiration systems under CO conditions

Other than Ni-CODHs and hydrogenases, anaerobic respiration genes required for energy production and conversion were identified as DEGs. In the presence of CO, the expression levels of gene clusters encoding periplasmic formate dehydrogenase (Fdh)-like proteins (KKC1_RS05300–KKC1_RS05315) and periplasmic nitrate reductase (Nap)-like proteins (KKC1_RS14135–KKC1_RS14170) were significantly upregulated, whereas those of a gene cluster encoding dissimilatory sulfite reductase (Dsr)-like proteins (KKC1_RS04115–KKC1_RS04185 and KKC1_RS04195) were downregulated (Fig. 2; Table 2 and S2). The Dsr complex couples sulfite reduction with a proton-translocating menaquinone cycle (Venceslau et al. 2014; Santos et al. 2015; Anantharaman et al. 2018), whereas Fdh and Nap couple formate oxidation with nitrate reduction to drive the menaquinone cycle (Fig. 2) (Richardson et al. 2004; Cerqueira et al. 2015). Under N_2 conditions, energy production is mainly performed through pyruvate oxidation and thiosulfate reduction (Yoneda et al. 2013). Our data suggested that the Dsr complex catalyzes electron transfer to the menaquinone pool by reducing the sulfite derived from thiosulfate in the absence of CO. Conversely, in the presence of CO, both Fdh- and Nap-like proteins would maintain the menaquinone cycle instead of Dsr, although authentic substrates of these proteins have not been identified.

Additionally, we found that the upregulated DEGs included three genes encoding the putative extracellular multiheme cytochromes *c* (MHCs; *mhc-1*, *mhc-2*, and *mhc-3*, corresponding to KKC1_RS04440, KKC1_RS08310, and KKC1_RS11980, respectively), which are responsible for redox cycles of metals including Fe(III), nitrogen compounds, and sulfur compounds by catalyzing electron transfer from/to quinone pools in the extracellular space (Mowat and Chapman 2005; Zhong and Shi 2018; Chong et al. 2018) (Fig. 2; Table 2 and S2). MHC-1, MHC-2, and MHC-3 have 12, 7, and 12 CX_2CH motifs capable of binding a heme moiety, respectively, and all three proteins were predicted to have N-terminal signal sequences for extracellular localization, indicating their involvement in extracellular electron transfer.

Carbon and nitrogen metabolism as a possible redox-buffering system in the CO response

Reducing equivalents from CO can be utilized for other redox metabolic pathways. In the presence of CO, genes encoding Kor-like proteins (KKC1_RS04895–KKC1_RS04910), a glutamine synthetase (GS)-like protein (KKC1_RS05230), and glutamate synthase (GOGAT)-like proteins (KKC1_RS05235–KKC1_RS05240) were identified as upregulated DEGs (Fig. 2; Table 3 and S2). Kor catalyzes the reversible conversion of succinyl-CoA to 2-oxoglutarate through (de)carboxylating reactions, using ferredoxin as an electron carrier (Fig. 2) (Yamamoto et al. 2010; Li and Elliott 2016; Chen et al. 2019). GOGAT produces two molecules of glutamate from 2-oxoglutarate and glutamine using NAD(P)H (Vanoni and Curti 2005), whereas GS produces glutamine from glutamate and ammonia using ATP (Eisenberg et al. 2000). It should be noted that a gene encoding a succinyl-CoA synthetase (SCS) μ subunit (KKC1_RS08680) was significantly downregulated in the presence of CO (Fig. 2; Table 3 and S2); however, *C. maritimus* KKC1 possesses three SCS gene sets, and the expression levels of the other two SCS genes were unchanged under CO conditions (Table S2).

Genes for a double-cubane cluster protein (DCCP), DCCP reductase (KKC1_RS14820–KKC1_RS14825), and

Table 2 List of anaerobic respiration machineries identified in DEGs

Functional group	Locus tag	Log_2FC	Annotation	COG number (category)[a]
Fdh	KKC1_RS05300	3.1	Twin-arginine translocase TatA/TatE family subunit	(U)
Fdh	KKC1_RS05305	3.7	FdoI	COG2864 (C)
Fdh	KKC1_RS05310	3.4	FdoH	COG0437 (C)
Fdh	KKC1_RS05315	3.7	FdoG	COG0243 (C)
Nap	KKC1_RS14135	5.8	Twin-arginine translocase TatA/TatE family subunit	(U)
Nap	KKC1_RS14140	5.8	NapD	
Nap	KKC1_RS14145	5.7	NapB	
Nap	KKC1_RS14150	5.9	NapG	COG1145 (C)
Nap	KKC1_RS14155	5.9	NapA	COG0243 (C)
Nap	KKC1_RS14160	5.7	Hypothetical protein (pseudogene)	
Nap	KKC1_RS14165	5.8	NapH	COG0348 (C)
Nap	KKC1_RS14170	5.8	NapG	COG1145 (C)
MHCs	KKC1_RS04440	7.7	MHC-1 ($12\times CX_2H$ motifs)	(S)
MHCs	KKC1_RS08310	7.9	MHC-2 ($7\times CX_2H$ motifs)	(S)
MHCs	KKC1_RS11980	3.2	MHC-3 ($12\times CX_2H$ motifs)	(C)
Dsr	KKC1_RS04115	−6.0	DsrT	(S)
Dsr	KKC1_RS04120	−5.7	DsrK	
Dsr	KKC1_RS04125	−6.1	DsrJ	(C)
Dsr	KKC1_RS04130	−5.0	DsrO	COG0437 (C)
Dsr	KKC1_RS04135	−5.8	DsrP	COG5557 (C)
Dsr	KKC1_RS04140	−5.5	DsrM	COG2181 (C)
Dsr	KKC1_RS04145	−6.0	DsrA	COG2221 (C)
Dsr	KKC1_RS04150	−6.1	DsrB	COG2221 (C)
Dsr	KKC1_RS04155	−6.7	DsrD	(S)
Dsr	KKC1_RS04160	−6.6	Ferredoxin	(C)
Dsr	KKC1_RS04165	−7.2	DsrC	COG2920 (P)
Dsr	KKC1_RS04170	−5.1	Pyridine nucleotide-disulphide oxidoreductase	COG0446,COG0607 (P)
Dsr	KKC1_RS04175	−5.3	DsrN	COG1797 (H)
Dsr	KKC1_RS04180	−6.2	DsrM	COG2181 (C)
Dsr	KKC1_RS04185	−6.1	DsrK	COG0247 (C)
Dsr	KKC1_RS04195	−2.8	DsrE	COG1416 (S)

[a]COG number and category were annotated by EggNOG mapper. Note that some COG categories were annotated, even when COG numbers were not annotated

FC fold change

an acyl carrier protein (KKC1_RS01055) were also identified as downregulated DEGs under CO conditions (Fig. 2; Table 3 and S2). DCCP and DCCP reductase represent a recently identified, novel, ATP-dependent oxidoreductase system in *C. hydrogenoformans* (Jeoung and Dobbek 2018) and the amino acid identities of DCCP and DCCP reductase homologs of *C. maritimus* KKC1 to those of *C. hydrogenoformans* were 57% and 41%, respectively. DCCP and DCCP reductase reduce acetylene to ethylene, with this activity inhibited by CO. Additionally, the acyl carrier protein plays a central role in fatty-acid biosynthesis, which requires the NADPH-dependent reduction of an acyl chain (Chan and Vogel 2010).

Transcription factors as DEGs

Putative transcription factors were also identified among the DEGs. Genes encoding two RocR-like AAA^+ superfamily transcriptional activators (KKC1_RS02905 and KKC1_RS04915) and one TetR/AcrR family transcriptional regulator (KKC1_RS07140) were upregulated in the presence of CO, whereas an LysR family transcriptional regulator (KKC1_RS14830) was downregulated (Table 4 and S2). To analyze the relationships between these transcription factors and their targets, the transcriptional units were predicted using the mapped RNA-seq data that included DEGs (Table S3). One gene encoding

Table 3 List of DEGs related to carbon and nitrogen metabolisms

Functional group	Locus tag	Log_2FC	Annotation	COG number (category)[a]
Kor	KKC1_RS04895	6.0	KorD	(C)
Kor	KKC1_RS04900	5.8	KorA	COG0674 (C)
Kor	KKC1_RS04905	5.8	KorB	COG1013 (C)
Kor	KKC1_RS04910	5.0	KorG	COG1014 (C)
GS/GOGAT	KKC1_RS05230	3.8	Glutamine synthetase	COG0174 (E)
GS/GOGAT	KKC1_RS05235	4.3	Glutamate synthase domain 1	COG0067 (E)
GS/GOGAT	KKC1_RS05240	3.3	Glutamate synthase domain 2	COG0069 (E)
SCS	KKC1_RS08680	− 6.4	Succinyl-CoA synthetase subunit alpha	COG0074 (C)
ACP	KKC1_RS01055	− 2.7	Acyl carrier protein	COG0236 (I)
DCCP	KKC1_RS14820	− 5.5	DCCP	COG1775 (E)
DCCP	KKC1_RS14825	− 4.5	DCCP reductase	COG1924 (I)

[a]COG number and category were annotated by EggNOG mapper. Note that some COG categories were annotated, even when COG numbers were not annotated

FC fold change

Table 4 List of transcription factors in DEGs

Functional group	Locus tag	Log_2FC	Annotation	COG number (category)[a]
RocR	KKC1_RS02905	3.3	RocR-like transcriptional activator	COG3829 (K)
RocR	KKC1_RS04915	4.7	RocR-like transcriptional activator	COG3829 (K)
TetR	KKC1_RS07140	2.8	TetR/AcrR family transcriptional regulator	(K)
LysR	KKC1_RS14830	− 2.9	LysR family transcriptional regulator	COG0583 (K)

[a]COG number and category were annotated by EggNOG mapper. Note that some COG categories were annotated, even when COG numbers were not annotated

FC fold change

an RocR-like protein (KKC1_RS04915) was adjacent to the *kor* genes, which were significantly upregulated, whereas the other gene (KKC1_RS02905) was an orphan. These two proteins shared 89% amino acid identity and possessed a conserved $HX_2CX_2CX_5C$ motif, possibly used for metal binding in the N-terminal sensor domain. RocR-like proteins were originally positive regulators of arginine catabolism in bacteria (Calogero et al. 1994). Genes encoding a TetR/AcrR-like protein and a LysR-like protein were located at transcriptional units encoding efflux transporter systems and DCCP/DCCP reductase, respectively (Tables S2 and S3). Moreover, our prediction of the transcriptional units revealed that two-component-system-like genes (KKC1_RS10605–KKC1_RS10610) were located in the unit containing *hyd-3b* genes, although these two-component-system-like genes were not identified as DEGs (Fig. 3a; Tables S2 and S3). These transcription factors might alter DEG expression levels in *C. maritimus* KKC1.

Transcription factor-binding motifs

To identify transcription-factor-binding motifs in the upstream regions of the DEGs, we searched for palindromic sequence motifs in the predicted transcriptional units (Table S3). Putative sequence motifs recognized by a CO-sensing transcriptional activator CooA and a redox-sensing transcriptional regulator Rex were identified in the transcriptional units upregulated by CO, whereas no transcription-factor-binding motif was identified in the downregulated transcriptional units (Fig. 3). A CooA-binding consensus sequence (5′-TGTC-N_8-GACA) was found in the upstream regions of the *cooS2–ech1* gene cluster and *cooS6*, as previously reported (Fig. 3a and b) (Omae et al. 2017), whereas Rex-binding sequence (5′-TTGTGA-N_6-TCACAA)-like motifs were found in the upstream regions of the transcriptional units containing the *cooS2–ech1*, *hyd-3b*, *kor*, *fdh*, and *nap* gene clusters and three *mhc* genes (Fig. 3a and c). These data implied that CooA and Rex are involved in the

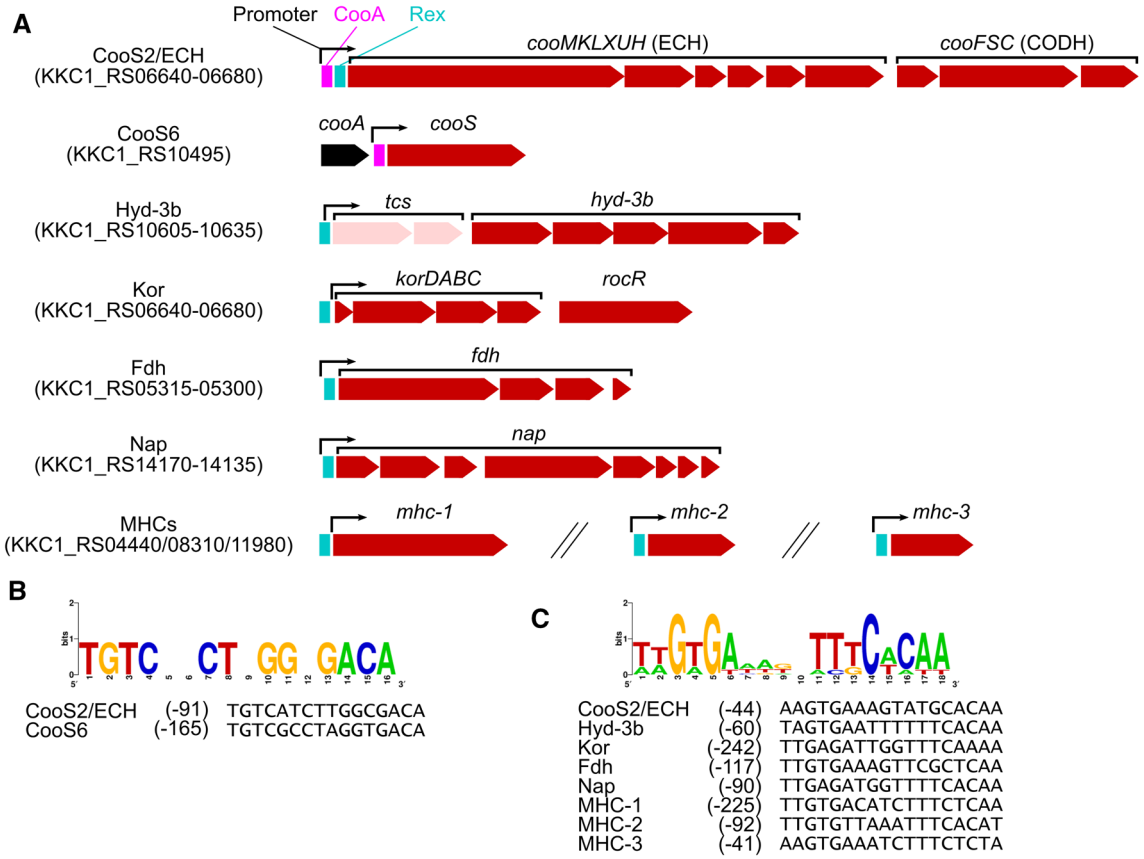

Fig. 3 Prediction of transcriptional response to CO in *C. maritimus* KKC1. **a** Predicted structure of CO-responsive transcriptional units regulated by CooA and Rex. The predicted promoter regions (−10 and −35 sequences) are indicated by arrows. Regions of sequence motifs recognized by CooA and Rex are colored magenta and cyan, respectively. Upregulated DEGs in the presence of CO and upregulated non-DEGs are colored red and pale red, respectively. The *cooA* gene, which is upstream of *cooS6*, is shown in black. *tcs*, two-component system genes. **b**,**c** Putative **b** CooA- and **c** Rex-binding sequence motifs. The sequence logo is shown above each sequence alignment, and the number of bases from the start codon is shown in parentheses

upregulation of these genes in the presence of CO in situations involving direct CO sensing and redox sensing, respectively.

Discussion

We examined transcriptomic changes in *C. maritimus* KKC1 growing in the presence or absence of CO using RNA-seq analysis. Our data showed that of the seven *cooS* genes and six hydrogenase genes studied, the *cooS2–ech1* (*coo*-type) gene cluster (not the *hyc*/*hyf*-type gene cluster), the "orphan" *cooS6* gene, and bidirectional *hyd-3b* genes were upregulated under CO condition (Fig. 2 and Table 1). In hydrogenogenic carboxydotrophic *Moorella* species, genes for the *hyc*/*hyf*-type hydrogenase form a gene cluster with *cooS* and are responsible for CO-dependent H_2 production (Poehlein et al. 2018; Fukuyama et al. 2019b), while in *Carboxydothermus* species, the *coo*-type works with *cooS* (Wu et al. 2005; Fukuyama et al. 2019a), suggesting that *C. maritimus* KKC1 utilizes a strategy similar to *Carboxydothermus* species rather than *Moorella* species for CO-dependent energy conservation. Upregulation of the "orphan" *cooS6* gene under CO conditions could induce the reduction of the ferredoxin pool and perturbation of cellular redox balance in *C. maritimus* KKC1. The bidirectional *hyd-3b* genes might balance such redox perturbation. Moreover, unlike *C. pertinax*, H_2-uptake *hyd-1a* genes were downregulated under CO conditions in *C. maritimus* KKC1 (Fig. 2 and Table 1) (Fukuyama et al. 2019a). These data suggest that an H_2-evolution system is predominant in the presence of CO because of the excessive reducing equivalents from CO in *C. maritimus* KKC1.

Our data support the broad usage of electron acceptors in anaerobic respiration of *C. maritimus* KKC1 (Fig. 2 and Table 2). We found that three *mhc* genes presumed to utilize Fe(III) were upregulated in the presence of CO. In *Thermincola potens*, MHCs are responsible for respiratory electron

transfer to Fe(III) (Carlson et al. 2012), and genomic analysis of *Carboxydocella thermoautotrophica* indicated the possible involvement of MHCs in CO-dependent Fe(III) reduction (Toshchakov et al. 2018). Similar to these hydrogenogenic carboxydotrophs, *C. maritimus* KKC1 produces Fe(II) with ferric citrate, amorphous Fe(III) oxide, and Fe_2O_3 in the presence of CO, suggesting that Fe(III) is used as an electron acceptor under CO conditions (Yoneda et al. 2013). Therefore, these MHCs might be responsible for extracellular electron transfer to Fe(III) in *C. maritimus* KKC1. On the contrary, *dsr* genes that utilize sulfite in thiosulfate respiration were downregulated in the presence of CO although *C. maritimus* KKC1 is considered to couple thiosulfate reduction with CO or pyruvate oxidation (Yoneda et al. 2013). Thiosulfate respiration is conducted by a concerted way of thiosulfate/polysulfide reductase (Phs) and Dsr (Stoffels et al. 2011; Venceslau et al. 2014). We could not identify any *phs* genes in *C. maritimus* KKC1; therefore, a complete thiosulfate reduction pathway in this organism remains unknown. *C. pertinax,* which can also utilize Fe(III) and thiosulfate with CO or pyruvate oxidation, shows that expressions of the *mhc*-like genes, the *dsr* gene cluster (cpu_17430–17,360), and the *phs* gene cluster (cpu_06910–06,930) remain unchanged between CO and N_2 conditions (Fukuyama et al. 2019a), suggesting that transcriptional responses in the anaerobic respiration pathway upon CO would differ between these two hydrogenogenic carboxydotrophs.

Oxidoreductase-like genes encoding Kor, GOGAT, and GS involved in carbon and nitrogen metabolisms were also upregulated under CO conditions in *C. maritimus* KKC1, strongly suggesting metabolic adaptation to cellular redox change upon CO oxidation (Fig. 2 and Table 3). Moreover, *kor* genes are upregulated in *Thermococcus onnurineus* under CO conditions, suggesting the possible involvement of Kor in carbon fixation (Moon et al. 2012), whereas the GS/GOGAT cycle is a redox-buffering system involving the consumption of NAD(P)H in *Caldicellulosiruptor bescii* and *Clostridium thermocellum* (Sander et al. 2015, 2019). It is possible that the enzymatic cycle involving Kor, GOGAT, and GS would assimilate carbon and nitrogen using excessive reducing equivalents from CO.

Additionally, we identified putative transcription factors as DEGs (Table 4) and putative CooA- and Rex-binding motifs in the upstream regions of upregulated DEGs (Fig. 3). As noted, the expression of *cooA* remained unchanged under CO conditions, suggesting that the basal expression level of *cooA* would be adequate to adapt to CO (Table S2). This phenomenon is different in *C. pertinax* and *Desulfovibrio vulgaris*, where *cooA* genes are upregulated in the presence of CO (Rajeev et al. 2012; Fukuyama et al. 2019a). Moreover, Rex is a redox-sensing transcriptional repressor and conserved among various bacteria, regardless of whether they are anaerobes or aerobes, and conformational changes from NAD^+- to NADH-bound states induce transcription by releasing Rex from its recognition sequence (McLaughlin et al. 2010; Ravcheev et al. 2012). *C. maritimus* KKC1 possesses one Rex homolog (KKC1_RS10865), which exhibits 39% and 41% amino acid identities with those from *C. bescii* and *Clostridium acetobutylicum*, respectively. As described here, *C. bescii* Rex regulates various types of hydrogenases including ECH, and pyruvate:ferredoxin oxidoreductase belonging to the same family as Kor (Sander et al. 2019). In *Clostridium* species, Rex regulates the expressions of genes encoding various types of oxidoreductase, including nitrate reductases, hydrogenases, and WLP enzymes (Zhang et al. 2014). Therefore, cellular redox changes under CO conditions in *C. maritimus* KKC1 might result in a high NADH/NAD^+ ratio to drive Rex-dependent transcriptional activation of oxidoreductase-like genes.

These findings suggest a possible multi-step transcriptional response to CO in *C. maritimus* KKC1 as follow: 1) upon CO exposure, CO-sensing CooA activates transcription of the *cooS2–ech1* gene cluster and *cooS6*, and these two Ni-CODHs catalyze CO oxidation to supply reducing equivalents within the cell; 2) excessive reducing equivalents from CO result in a high NADH/NAD^+ ratio, followed by Rex-dependent transcriptional activation of the *cooS2–ech1*, *hyd-3b*, *kor*, *fdh,* and *nap* gene clusters, and three *mhc* genes; and 3) changes in the metabolisms or expression of transcription factors induce alterations in the transcription of other DEGs.

Our data highlight the diversity of CO-responsive transcriptional regulation in thermophilic, hydrogenogenic, carboxydotrophic bacteria. In *C. pertinax*, of the nine gene clusters upregulated in the presence of CO, including *cooS*, only the *ech* gene cluster is directly regulated by CooA (Fukuyama et al. 2019a), whereas the Rex-binding motif or those of other transcription factors are not found in upstream regions of these nine gene clusters. Additionally, in hydrogenogenic, carboxydotrophic *Moorella* strains, whose genomes encode no known CO-sensing transcription factor homologs, genes for RocR-like transcriptional activators (MOST_RS16225 in *M. stamsii* and MOTE_RS04420 in *M. thermoacetica* DSM 21,394) are located in the upstream regions of their Ni-CODH–ECH gene clusters. Because two genes for RocR-like proteins were upregulated under CO condition in *C. maritimus* KKC1 (Table 4), RocR-like proteins related to Ni-CODH–ECH gene clusters in these two *Moorella* species might be involved in response to CO. Moreover, a recent comparative genomics study of *Parageobacillus thermoglucosidasius*, a hydrogenogenic carboxydotroph also lacking known CO-sensing transcription factors, has found a transition-state regulator Hpr-binding sequence in the upstream region of its Ni-CODH–ECH gene cluster (Mohr et al. 2018). These findings imply previously undescribed

transcriptional response mechanisms to CO. There could be various ways to respond to CO, including directly sensing CO, via stress caused by CO, or through cellular redox or metabolic changes via CO oxidation. Therefore, the diverse strategies for adaptation to CO-dependent metabolism would have been evolved in thermophilic, hydrogenogenic, carboxydotrophic bacteria.

Acknowledgements Computation time was provided by the Super-Computer System, Institute for Chemical Research, Kyoto University. The work was supported by JSPS KAKENHI Grant Number JP16H06381 (to Y.S.). M.I., T.Y., and Y.S. conceived and designed the study. M.I. and H.I. performed the RNA-seq and RT-ddPCR experiments and data analysis. M.I., T.Y., and Y.S. wrote the manuscript with the assistance of H.I., Y.F., and K.O. All of the authors reviewed and approved the manuscript.

Compliance with ethical standards

Conflict of interest The authors declare no conflict of interest.

Open Access This article is licensed under a Creative Commons Attribution 4.0 International License, which permits use, sharing, adaptation, distribution and reproduction in any medium or format, as long as you give appropriate credit to the original author(s) and the source, provide a link to the Creative Commons licence, and indicate if changes were made. The images or other third party material in this article are included in the article's Creative Commons licence, unless indicated otherwise in a credit line to the material. If material is not included in the article's Creative Commons licence and your intended use is not permitted by statutory regulation or exceeds the permitted use, you will need to obtain permission directly from the copyright holder. To view a copy of this licence, visit http://creativecommons.org/licenses/by/4.0/.

References

Almagro Armenteros JJ, Tsirigos KD, Sønderby CK et al (2019) SignalP 5.0 improves signal peptide predictions using deep neural networks. Nat Biotechnol 37:420–423. https://doi.org/10.1038/s41587-019-0036-z

Alves JI, van Gelder AH, Alves MM et al (2013) *Moorella stamsii* sp. nov., a new anaerobic thermophilic hydrogenogenic carboxydotroph isolated from digester sludge. Int J Syst Evol Microbiol 63:4072–4076. https://doi.org/10.1099/ijs.0.050369-0

Anantharaman K, Hausmann B, Jungbluth SP et al (2018) Expanded diversity of microbial groups that shape the dissimilatory sulfur cycle. ISME J 12:1715–1728. https://doi.org/10.1038/s41396-018-0078-0

Bailey TL, Boden M, Buske FA et al (2009) MEME SUITE: tools for motif discovery and searching. Nucleic Acids Res 37:W202–W208. https://doi.org/10.1093/nar/gkp335

Brettin T, Davis JJ, Disz T et al (2015) *RASTtk*: A modular and extensible implementation of the RAST algorithm for building custom annotation pipelines and annotating batches of genomes. Sci Rep 5:8365. https://doi.org/10.1038/srep08365

Calogero S, Gardan R, Glaser P et al (1994) RocR, a novel regulatory protein controlling arginine utilization in *Bacillus subtilis*, belongs to the NtrC/NifA family of transcriptional activators. J Bacteriol 176:1234–1241. https://doi.org/10.1128/jb.176.5.1234-1241.1994

Camacho C, Coulouris G, Avagyan V et al (2009) BLAST+: Architecture and applications. BMC Bioinformatics 10:421. https://doi.org/10.1186/1471-2105-10-421

Can M, Armstrong FA, Ragsdale SW (2014) Structure, function, and mechanism of the nickel metalloenzymes, CO dehydrogenase, and acetyl-CoA synthase. Chem Rev 114:4149–4174. https://doi.org/10.1021/cr400461p

Carlson HK, Iavarone AT, Gorur A et al (2012) Surface multiheme *c*-type cytochromes from *Thermincola potens* and implications for respiratory metal reduction by Gram-positive bacteria. Proc Natl Acad Sci USA 109:1702–1707. https://doi.org/10.1073/pnas.1112905109

Cerqueira NMFSA, Gonzalez PJ, Fernandes PA et al (2015) Periplasmic nitrate reductase and formate dehydrogenase: similar molecular architectures with very different enzymatic activities. Acc Chem Res 48:2875–2884. https://doi.org/10.1021/acs.accounts.5b00333

Chan DI, Vogel HJ (2010) Current understanding of fatty acid biosynthesis and the acyl carrier protein. Biochem J 430:1–19. https://doi.org/10.1042/BJ20100462

Chen PYT, Li B, Drennan CL, Elliott SJ (2019) A reverse TCA cycle 2-oxoacid: ferredoxin oxidoreductase that makes C-C bonds from CO_2. Joule 3:595–611. https://doi.org/10.1016/j.joule.2018.12.006

Chong GW, Karbelkar AA, El-Naggar MY (2018) Nature's conductors: what can microbial multi-heme cytochromes teach us about electron transport and biological energy conversion? Curr Opin Chem Biol 47:7–17. https://doi.org/10.1016/j.cbpa.2018.06.007

Crooks GE, Hon G, Chandonia JM, Brenner SE (2004) WebLogo: A Sequence Logo Generator. Genome Res 14:1188–1190. https://doi.org/10.1101/gr.849004

Diender M, Stams AJM, Sousa DZ (2015) Pathways and bioenergetics of anaerobic carbon monoxide fermentation. Front Microbiol 6:1275. https://doi.org/10.3389/fmicb.2015.01275

Drake HL, Daniel SL (2004) Physiology of the thermophilic acetogen *Moorella thermoacetica*. Res Microbiol 155:869–883. https://doi.org/10.1016/j.resmic.2004.10.002

Eisenberg D, Gill HS, Pfluegl GMU, Rotstein SH (2000) Structure-function relationships of glutamine synthetases. Biochim Biophys Acta - Protein Struct Mol Enzymol 1477:122–145. https://doi.org/10.1016/S0167-4838(99)00270-8

Fukuyama Y, Omae K, Yoneda Y et al (2018) Insight into energy conservation via alternative carbon monoxide metabolism in *Carboxydothermus pertinax* revealed by comparative genome analysis. Appl Environ Microbiol 84:e00458-18. https://doi.org/10.1128/aem.00458-18

Fukuyama Y, Omae K, Yoshida T, Sako Y (2019a) Transcriptome analysis of a thermophilic and hydrogenogenic carboxydotroph *Carboxydothermus pertinax*. Extremophiles 23:389–398. https://doi.org/10.1007/s00792-019-01091-x

Fukuyama Y, Tanimura A, Inoue M et al (2019b) Draft genome sequences of two Thermophilic *Moorella* sp. strains, isolated from an acidic hot spring in Japan. Microbiol Resour Announc 8:e00663-19. https://doi.org/10.1128/MRA.00663-19

Galperin MY, Makarova KS, Wolf YI, Koonin EV (2015) Expanded microbial genome coverage and improved protein family annotation in the COG database. Nucleic Acids Res 43:D261–D269. https://doi.org/10.1093/nar/gku1223

Greening C, Biswas A, Carere CR et al (2016) Genomic and metagenomic surveys of hydrogenase distribution indicate H_2 is a widely utilised energy source for microbial growth and survival. ISME J 10:761–777. https://doi.org/10.1038/ismej.2015.153

Hille R, Dingwall S, Wilcoxen J (2015) The aerobic CO dehydrogenase from *Oligotropha carboxidovorans*. J Biol Inorg Chem 20:243–251. https://doi.org/10.1007/s00775-014-1188-4

Huerta-Cepas J, Forslund K, Coelho LP et al (2017) Fast genome-wide functional annotation through orthology assignment by

eggNOG-Mapper. Mol Biol Evol 34:2115–2122. https://doi.org/10.1093/molbev/msx148

Inoue M, Nakamoto I, Omae K et al (2019) Structural and phylogenetic diversity of anaerobic carbon-monoxide dehydrogenases. Front Microbiol 9:3353. https://doi.org/10.3389/fmicb.2018.03353

Jeoung J-H, Dobbek H (2018) ATP-dependent substrate reduction at an [Fe_8S_9] double-cubane cluster. Proc Natl Acad Sci USA 115:2994–2999. https://doi.org/10.1073/pnas.1720489115

Kanehisa M, Goto S, Sato Y et al (2012) KEGG for integration and interpretation of large-scale molecular data sets. Nucleic Acids Res 40:D109–D114. https://doi.org/10.1093/nar/gkr988

Kerby RL, Youn H, Roberts GP (2008) RcoM: A new single-component transcriptional regulator of CO metabolism in bacteria. J Bacteriol 190:3336–3343. https://doi.org/10.1128/JB.00033-08

Kim D, Langmead B, Salzberg SL (2015) HISAT: a fast spliced aligner with low memory requirements. Nat Methods 12:357–360. https://doi.org/10.1038/nmeth.3317

Komori H, Inagaki S, Yoshioka S et al (2007) Crystal structure of CO-sensing transcription activator CooA bound to exogenous ligand imidazole. J Mol Biol 367:864–871. https://doi.org/10.1016/j.jmb.2007.01.043

Li B, Elliott SJ (2016) The catalytic bias of 2-oxoacid:ferredoxin oxidoreductase in CO_2: evolution and reduction through a ferredoxin-mediated electrocatalytic assay. Electrochim Acta 199:349–356. https://doi.org/10.1016/j.electacta.2016.02.119

Li H, Handsaker B, Wysoker A et al (2009) The sequence alignment/map format and SAMtools. Bioinformatics 25:2078–2079. https://doi.org/10.1093/bioinformatics/btp352

Liao Y, Smyth GK, Shi W (2014) featureCounts: an efficient general purpose program for assigning sequence reads to genomic features. Bioinformatics 30:923–930. https://doi.org/10.1093/bioinformatics/btt656

McLaughlin KJ, Strain-Damerell CM, Xie K et al (2010) Structural basis for NADH/NAD^+ redox sensing by a rex family repressor. Mol Cell 38:563–575. https://doi.org/10.1016/j.molcel.2010.05.006

Mohr T, Aliyu H, Küchlin R et al (2018) Comparative genomic analysis of *Parageobacillus thermoglucosidasius* strains with distinct hydrogenogenic capacities. BMC Genomics 19:880. https://doi.org/10.1186/s12864-018-5302-9

Moon Y-J, Kwon J, Yun S-H et al (2012) Proteome analyses of hydrogen-producing hyperthermophilic archaeon *Thermococcus onnurineus* NA1 in different one-carbon substrate culture conditions. Mol Cell Proteomics 11:M111.015420. https://doi.org/10.1074/mcp.m111.015420

Mowat CG, Chapman SK (2005) Multi-heme cytochromes—new structures, new chemistry. Dalt Trans 2005:3381–3389. https://doi.org/10.1039/b505184c

NCBI Resource Coordinators (2018) Database resources of the national center for biotechnology information. Nucleic Acids Res 46:D8–D13. https://doi.org/10.1093/nar/gkx1095

Oelgeschläger E, Rother M (2008) Carbon monoxide-dependent energy metabolism in anaerobic bacteria and archaea. Arch Microbiol 190:257–269. https://doi.org/10.1007/s00203-008-0382-6

Omae K, Yoneda Y, Fukuyama Y et al (2017) Genomic analysis of *Calderihabitans maritimus* KKC1, a thermophilic, hydrogenogenic, carboxydotrophic bacterium isolated from marine sediment. Appl Environ Microbiol 83:e00832-17. https://doi.org/10.1128/AEM.00832-17

Pfennig N, Lippert KD (1966) Über das Vitamin B12-Bedürfnis phototropher Schwefelbakterien. Arch Mikrobiol 55:245–256. https://doi.org/10.1007/BF00410246

Poehlein A, Böer T, Steensen K, Daniel R (2018) Draft genome sequence of the hydrogenogenic carboxydotroph *Moorella stamsii* DSM 26271. Genome Announc 6:e00345-18. https://doi.org/10.1128/genomea.00345-18

Ragsdale SW (2004) Life with carbon monoxide. Crit Rev Biochem Mol Biol 39:165–195. https://doi.org/10.1080/10409230490496577

Rajeev L, Hillesland KL, Zane GM et al (2012) Deletion of the *Desulfovibrio vulgaris* carbon monoxide sensor invokes global changes in transcription. J Bacteriol 194:5783–5793. https://doi.org/10.1128/JB.00749-12

Ravcheev DA, Li X, Latif H et al (2012) Transcriptional regulation of central carbon and energy metabolism in bacteria by redox-responsive repressor rex. J Bacteriol 194:1145–1157. https://doi.org/10.1128/JB.06412-11

Richardson DJ, Sawers G, Van Spanning RJM (2004) Periplasmic Electron Transport Systems in Bacteria. In: Lennarz WJ, Lane MD (eds) Encyclopedia of Biological Chemistry. Elsevier, New York, pp 231–238

Robinson MD, McCarthy DJ, Smyth GK (2009) edgeR: a Bioconductor package for differential expression analysis of digital gene expression data. Bioinformatics 26:139–140. https://doi.org/10.1093/bioinformatics/btp616

Sander K, Chung D, Hyatt D et al (2019) Rex in *Caldicellulosiruptor bescii*: Novel regulon members and its effect on the production of ethanol and overflow metabolites. Microbiologyopen 8:e00639. https://doi.org/10.1002/mbo3.639

Sander K, Wilson CM, Rodriguez M et al (2015) *Clostridium thermocellum* DSM 1313 transcriptional responses to redox perturbation. Biotechnol Biofuels 8:211. https://doi.org/10.1186/s13068-015-0394-9

Santos AA, Venceslau SS, Grein F et al (2015) A protein trisulfide couples dissimilatory sulfate reduction to energy conservation. Science 350:1541–1545. https://doi.org/10.1126/science.aad3558

Schoelmerich MC, Müller V (2019) Energy conservation by a hydrogenase-dependent chemiosmotic mechanism in an ancient metabolic pathway. Proc Natl Acad Sci USA 116:6329–6334. https://doi.org/10.1073/pnas.1818580116

Schut GJ, Lipscomb GL, Nguyen DMN et al (2016) Heterologous production of an energy-conserving carbon monoxide dehydrogenase complex in the hyperthermophile *Pyrococcus furiosus*. Front Microbiol 7:29. https://doi.org/10.3389/fmicb.2016.00029

Shelver D, Kerby RL, He Y, Roberts GP (1995) Carbon monoxide-induced activation of gene expression in *Rhodospirillum rubrum* requires the product of *cooA*, a member of the cyclic AMP receptor protein family of transcriptional regulators. J Bacteriol 177:2157–2163. https://doi.org/10.1128/jb.177.8.2157-2163.1995

Shin J, Song Y, Jeong Y, Cho BK (2016) Analysis of the core genome and pan-genome of autotrophic acetogenic bacteria. Front Microbiol 7:1531. https://doi.org/10.3389/fmicb.2016.01531

Singer SW, Hirst MB, Ludden PW (2006) CO-dependent H_2 evolution by *Rhodospirillum rubrum*: role of CODH:CooF complex. Biochim Biophys Acta - Bioenerg 1757:1582–1591. https://doi.org/10.1016/j.bbabio.2006.10.003

Soboh B, Linder D, Hedderich R (2002) Purification and catalytic properties of a CO-oxidizing:H_2-evolving enzyme complex from *Carboxydothermus hydrogenoformans*. Eur J Biochem 269:5712–5721. https://doi.org/10.1046/j.1432-1033.2002.03282.x

Sokolova TG, Henstra AM, Sipma J et al (2009) Diversity and ecophysiological features of thermophilic carboxydotrophic anaerobes. FEMS Microbiol Ecol 68:131–141. https://doi.org/10.1111/j.1574-6941.2009.00663.x

Søndergaard D, Pedersen CNS, Greening C (2016) HydDB: A web tool for hydrogenase classification and analysis. Sci Rep 6:34212. https://doi.org/10.1038/srep34212

Stoffels L, Krehenbrink M, Berks BC et al (2011) Thiosulfate reduction in *Salmonella enterica* is driven by the proton motive force. J Bacteriol 194:475–485. https://doi.org/10.1128/JB.06014-11

Svetlichny VA, Sokolova TG, Gerhardt M et al (1991) *Carboxydothermus hydrogenoformans* gen. nov., sp. nov., a CO-utilizing thermophilic anaerobic bacterium from hydrothermal environments of Kunashir Island. Syst Appl Microbiol 14:254–260. https://doi.org/10.1016/S0723-2020(11)80377-2

Techtmann SM, Colman AS, Robb FT (2009) 'That which does not kill us only makes us stronger': the role of carbon monoxide in thermophilic microbial consortia. Environ Microbiol 11:1027–1037. https://doi.org/10.1111/j.1462-2920.2009.01865.x

Techtmann SM, Lebedinsky AV, Colman AS et al (2012) Evidence for horizontal gene transfer of anaerobic carbon monoxide dehydrogenases. Front Microbiol 3:132. https://doi.org/10.3389/fmicb.2012.00132

Thorvaldsdóttir H, Robinson JT, Mesirov JP (2013) Integrative genomics viewer (IGV): high-performance genomics data visualization and exploration. Brief Bioinform 14:178–192. https://doi.org/10.1093/bib/bbs017

Toshchakov SV, Lebedinsky AV, Sokolova TG et al (2018) Genomic insights into energy metabolism of *Carboxydocella thermautotrophica* coupling hydrogenogenic CO oxidation with the reduction of Fe(III) minerals. Front Microbiol 9:1759. https://doi.org/10.3389/fmicb.2018.01759

Vanoni MA, Curti B (2005) Structure–function studies on the iron–sulfur flavoenzyme glutamate synthase: an unexpectedly complex self-regulated enzyme. Arch Biochem Biophys 433:193–211. https://doi.org/10.1016/j.abb.2004.08.033

Venceslau SS, Stockdreher Y, Dahl C, Pereira IAC (2014) The "bacterial heterodisulfide" DsrC is a key protein in dissimilatory sulfur metabolism. Biochim Biophys Acta - Bioenerg 1837:1148–1164. https://doi.org/10.1016/j.bbabio.2014.03.007

Wolin EA, Wolin MJ, Wolfe RS (1963) Formation of methane by bacterial extracts. J Biol Chem 238:2882–2886

Wu M, Ren Q, Durkin AS et al (2005) Life in hot carbon monoxide: the complete genome sequence of *Carboxydothermus hydrogenoformans* Z-2901. PLoS Genet 1:e65. https://doi.org/10.1371/journal.pgen.0010065

Yamamoto M, Ikeda T, Arai H et al (2010) Carboxylation reaction catalyzed by 2-oxoglutarate:ferredoxin oxidoreductases from *Hydrogenobacter thermophilus*. Extremophiles 14:79–85. https://doi.org/10.1007/s00792-009-0289-4

Yoneda Y, Yoshida T, Yasuda H et al (2013) A thermophilic, hydrogenogenic and carboxydotrophic bacterium, *Calderihabitans maritimus* gen. nov., sp. nov., from a marine sediment core of an undersea caldera. Int J Syst Evol Microbiol 63:3602–3608. https://doi.org/10.1099/ijs.0.050468-0

Zhang L, Nie X, Ravcheev DA et al (2014) Redox-responsive repressor rex modulates alcohol production and oxidative stress tolerance in *Clostridium acetobutylicum*. J Bacteriol 196:3949–3963. https://doi.org/10.1128/JB.02037-14

Zhong Y, Shi L (2018) Genomic analyses of the quinol oxidases and/or quinone reductases involved in bacterial extracellular electron transfer. Front Microbiol 9:3029. https://doi.org/10.3389/fmicb.2018.03029

Publisher's Note Springer Nature remains neutral with regard to jurisdictional claims in published maps and institutional affiliations.